Obrabotka metallov (tekhnologiya, oborudovanie, instrumenty) = Metal Working and Material Science. 2026 vol. 28 no. 2 pp. 335–350
ISSN: 1994-6309 (print) / 2541-819X (online)
DOI: 10.17212/1994-6309-2026-28.2-335-350

NSTU NETI

Obrabotka metallov -
Metal Working and Material Science

Journal homepage: http://journals.nstu.ru/obrabotka_metallov

Analysis of temperature–strain processes during explosive welding of the 1050A / 321 composite using numerical simulation

Yulia Malyutina [1, 2, a, *], *Tatyana Ogneva* [1, b], *Ivan Bataev* [1, c], *Elena Lozhkina* [1, d], *Vladimir Pai* [2, e], *Yaroslav Lukyanov* [2, f], *Evgeny Kuzmin* [3, j]

[1] Novosibirsk State Technical University, 20 Prospekt K. Marksa, Novosibirsk, 630073, Russian Federation
[2] Lavrentyev Institute of Hydrodynamics SB RAS, 15 Akademika Lavrentyev Ave., Novosibirsk, 630090, Russian Federation
[3] Volgograd State Technical University, 28 V.I. Lenin, Volgograd, 400005, Russian Federation

[a] https://orcid.org/0000-0002-0305-7518, iuliiamaliutina@gmail.com; [b] https://orcid.org/0000-0002-0081-283X, pandorra.06@mail.ru;
[c] https://orcid.org/0000-0003-2871-0269, ivanbataev@ngs.ru; [d] https://orcid.org/0000-0002-7119-4944, lozhkinaelena1987@gmail.com;
[e] https://orcid.org/0009-0009-3819-8431, pai@hydro.nsc.ru; [f] https://orcid.org/0000-0003-4526-9399, lukyanov@hydro.nsc.ru;
[j] https://orcid.org/0000-0002-1037-5186, e.v.kuzmin@yandex.ru

ARTICLE INFO

Article history:
Received: 08 April 2026
Revised: 16 April 2026
Accepted: 30 April 2026
Available online: 15 June 2026

Keywords:
Explosive welding
SPH method
Aluminum
Stainless steel
Impact angle

Funding
This research was supported by grant No. 25-23-01117 from the Russian Science Foundation, https://rscf.ru/project/25-23-01117/.

Acknowledgements
The research was conducted using equipment at the Center for Collective Use “Structure, Mechanical, and Physical Properties of Materials” (NSTU).

ABSTRACT

Traditional welding methods are rarely used to join such material pairs due to their tendency to form brittle intermetallic compounds. One of the main parameters determining the quality of the weld is the impact angle γ. ***The aim of the work*** is to study the influence of the impact angle on the temperature-strain characteristics in the joint zone during high-velocity impact of aluminum *1050A* and steel *321* plates using numerical simulation. **Research methods.** The smoothed particle hydrodynamics (*SPH*) method implemented in *Ansys Autodyn 2020 R2* software was used for the simulations. In all calculations, the contact point velocity was constant at V_c = 2,500 m/s, and the impact angle varied (9.5°, 12°, 14.5°). The *Mie–Grüneisen* equation of state and the *Johnson–Cook* constitutive model were used to describe the properties of the materials. **Results and discussion.** It was found that an increase in the impact angle leads to higher pressure, temperature, and plastic strain. Specifically, temperature and plastic strain increase monotonically with γ, whereas pressure varies non-monotonically, reaching a peak of 8.87 GPa at γ = 12°. At γ = 12°, the most uniform interface is formed, and at γ = 14.5°, an asymmetrical interface with the penetration of steel into aluminum is observed. All studied impact conditions result in local melting of aluminum while keeping the steel solid. The most favorable of the investigated impact angles, which provides a beneficial combination of pressure, temperature, and interface morphology for the *1050A/321* system at a speed of 2,500 m/s, is 12°.

For citation: Malyutina Yu.N., Ogneva T.S., Bataev I.A., Lozhkina E.A., Pai V.V., Lukyanov Ya.L., Kuzmin E.V. Analysis of temperature–strain processes during explosive welding of the 1050A / 321 composite using numerical simulation. *Obrabotka metallov (tekhnologiya, oborudovanie, instrumenty) = Metal Working and Material Science*, 2026, vol. 28, no. 2, pp. 335–350. DOI: 10.17212/1994-6309-2026-28.2-335-350. (In Russian).

*** Corresponding author**
Malyutina Yuliya N., PhD (Engineering), Associate Professor
Novosibirsk State Technical University,
20 Prospekt K. Marksa,
630073, Novosibirsk, Russian Federation
Tel.: +7 913 476-99-90, **e-mail:** iuliiamaliutina@gmail.com

Introduction

Explosive welding is one of the most effective methods for joining dissimilar materials, in particular, aluminum–steel composites [1–3]. Bimetals of this type are widely used in chemical engineering, shipbuilding, and the power industry due to the combination of high strength and low cost of steel with the low density, high thermal conductivity, and electrical conductivity of aluminum [4–6]. However, joining these materials by conventional fusion welding methods is difficult because of the formation of brittle intermetallic compounds (*FeAl*, Fe_3Al, etc.), which sharply reduce the strength of the weld.

Several studies have been devoted to the experimental investigation of explosive welding of aluminum–stainless steel pairs [7–12]. In the work of *B.S. Zlobin*, an analysis of the kinematic parameters determining the onset of bonding during oblique impact of aluminum and steel plates was carried out, and experimental data on material flow in the gap between the colliding plates were presented [7]. The formation of intermetallic compounds in aluminum–steel bimetals produced by explosive welding was addressed in [13–15]. It was established that heat treatment of explosively welded composites leads to the formation of brittle intermetallic compounds of various stoichiometric compositions, which significantly reduce the joint strength.

The explosive welding process is based on high-velocity impact of the workpieces, which is characterized by large plastic deformations and localized heat release. One of the main parameters determining the nature of plastic flow in the joint zone and, consequently, the weld quality, is the impact angle (γ) [12]. The weld morphology, jet shape, and temperature–strain conditions of joint formation depend on this angle [16, 17]. *F. Grignon* et al. [16] demonstrated experimentally and numerically that for aluminum-to-aluminum explosive welding, small impact angles ($\gamma = 4°$) result in a flat interface, whereas increasing the angle to 14° leads to a wavy interface morphology.

Numerical simulation studies have shown that the impact angle determines the contact pressure, shear stresses, and the magnitude of plastic strain [17]. At the macroscale, the pressure distribution near the collision point strongly depends on the impact velocity. This velocity, in turn, is determined by both the flyer plate velocity and the impact angle γ. Thus, the impact parameters significantly influence the distribution of temperature and strain fields in the joint zone. At the nanoscale, the impact parameters affect dislocation slip and diffusion processes [17].

Experimental determination of temperature, strain rate, and strain level during high-velocity impact is extremely challenging and often impossible. One of the few works in this field was reported by *V.V. Pay* et al., in which temperature was measured during explosive compaction using a natural thermocouple method [18]. Despite the emergence of such experimental approaches, numerical simulation remains an effective tool for studying the features of the high-velocity impact process. In recent years, the meshfree smoothed particle hydrodynamics (*SPH*) method has been widely used to model problems involving large plastic deformations [19–21]. The work of *S. Tanaka* and *K. Hokamoto's* group demonstrated that the *SPH* method can accurately reproduce the formation of wavy interfaces, vortex zones, and cumulative jets, as well as correctly describe the impact kinematics [22, 23]. Nevertheless, a systematic analysis of the influence of the impact angle on the full set of thermomechanical characteristics for the *1050A* / *321* pair is insufficiently represented in the literature, and obtaining such quantitative relationships constitutes the scientific novelty of the present work.

The aim of this work is to investigate the influence of the impact angle on the temperature and strain characteristics of the explosive welding process for *1050A* aluminum and *321* stainless steel during high-velocity impact using numerical simulation with the *SPH* method.

To achieve this aim, the following ***tasks*** were addressed:

– development of a two-dimensional model of the explosive welding process for the *1050A* / *321* composite using the *SPH* method in the *Ansys Autodyn* software, at a collision point velocity of 2,500 m/s and impact angles of 9.5°, 12°, and 14.5°;

– investigation of the interface morphology as a function of the impact angle;

– analysis of the influence of the impact angle on pressure, temperature, effective plastic strain, and strain rate in the joint zone;

– determination of the optimal impact angle that ensures the formation of a high-quality bimetal joint.

Research methodology

Numerical simulation was performed using the *Ansys Autodyn 2020 R2* software package with the *SPH* method, which is widely used for simulation of explosive welding [24, 25]. The simulations were carried out in a two-dimensional formulation. A schematic of the computational domain is shown in Fig. 1. The flyer plate was made of *1050A* aluminum alloy (*Al*) with dimensions of 2 × 15 mm. The base plate, measuring 1 × 15 mm, was made of *321* stainless steel (*SS*). The collision point velocity was kept constant at V_c = 2,500 m/s in all cases. The impact angle **γ** was varied from 9.5° to 14.5° in steps of 2.5°. The initial temperature of all particles was set to 293 K. To determine the appropriate *SPH* particle size, a series of simulations was conducted with particle sizes ranging from 7.5 to 200 µm. Analysis of the system's internal energy showed that at particle sizes of 10 µm and below, the energy values stabilized within less than 5%, indicating satisfactory convergence. Accordingly, a particle size of 10 µm was adopted for this study, with a total of 450,000 particles.

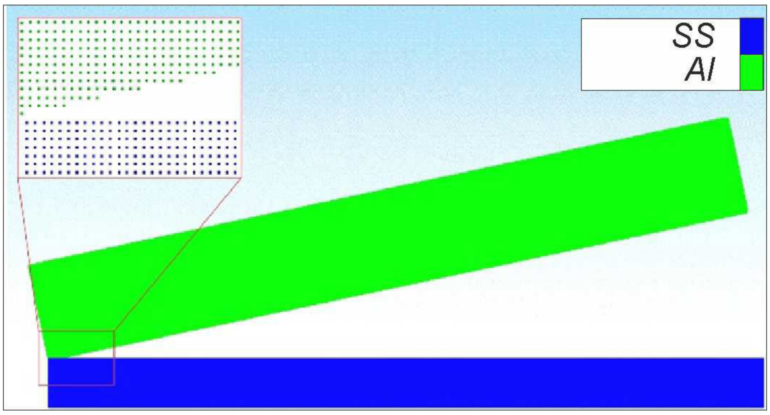

Fig. 1. Computational domain before the collision

The kinematic impact parameters were determined based on a geometric analysis of the parallel welding scheme using formulas given in [26] and were used to prescribe the initial conditions for the simulations. Free boundary conditions were applied to the outer surfaces of the plates, which is a standard approach in problems of high-velocity glancing impact and helps to avoid distortions caused by reflected waves.

The modified *Mie–Grüneisen* equation of state was used in this study, and the *Johnson–Cook* model was employed as the constitutive model. Both models are implemented in *Ansys Autodyn* and are widely used for simulating high-velocity impact processes accompanied by large plastic deformations [27]. The material constants used in the *Johnson–Cook* equation and the *Mie–Grüneisen* equation of state are presented in Tables 1 and 2.

Table 1

Parameters of *Mie-Grüneisen* equation of state [28–30]

Material	Initial density ρ_0, g/cm^3	*Grüneisen* coefficient, G_0	Parameter *C1*, m/ms	Parameter *S1*	Initial temperature, T_{room}, K	Specific heat capacity c_v, kJ/g×K
*Aluminium 1050*A	2.712	1.14	5.45	1.25	293	$8.84 \cdot 10^{-4}$
Steel 321	7.9	1.93	4.57	1.49	293	$4.23 \cdot 10^{-4}$

Table 2

Parameters of the *Johnson-Cook* strength model [28, 29, 31]

Material	*Al* (*1050A aluminium*)	*SS* (*321 steel*)
Shear modulus ***G***, GPa	27.6	78
Initial yield strength ***A***, GPa	0.1484	0.31
Hardening constant ***B***, GPa	0.3455	1
Exponent ***n***	0.183	0.65
Strain rate constant ***C***	0.001	0.07
Exponent ***m***	0.895	1
Melting point T_{melt}, K	929	1673
Initial strain rate (/s)	1	1
Strain rate correction	1^{st} Order	1^{st} Order

To assess the influence of the impact angle on the temperature and deformation processes, a series of calculations was performed with a constant collision point velocity V_c = 2,500 m/s and various impact angles γ (9.5°, 12°, and 14.5°). The following parameters were analyzed during the simulations: temperature, pressure, effective plastic strain, and strain rate in the impact zone.

Results and discussion

This section presents the results of numerical simulation of the high-velocity impact of *1050A* aluminum and *321* steel plates at different impact angles γ (9.5°, 12°, and 14.5°). The analysis was performed based on the weld joint morphology (Fig. 2), the distributions of pressure, temperature, effective plastic strain, and strain rate (Figs. 3, 4), as well as their time dependences (Figs. 5, 6).

Fig. 2 shows the features of interface formation during high-velocity impact of *1050A* aluminum (shown in green) and *321* steel (shown in blue) plates for three impact angles, γ = 9.5° (Fig. 2,*a–a2*), 12° (Fig. 2, *b–b2*), and 14.5° (Fig. 2, *c–c2*), at successive time instants.

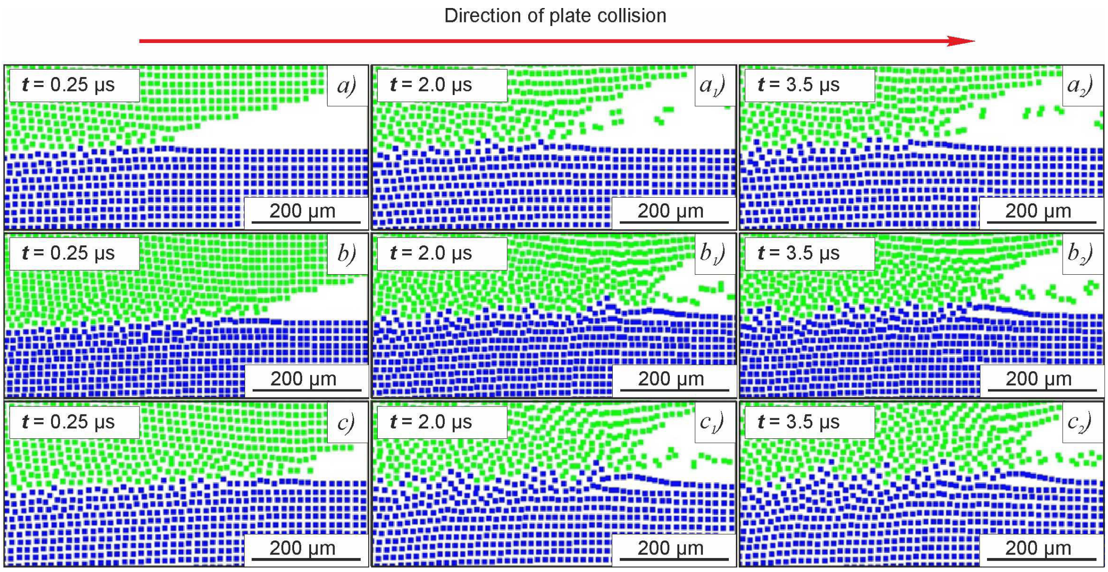

Fig. 2. Formation of the interface relief during collision of plates at different moments in time:

a–a$_2$ – 9.5°; *b–b*$_2$ – 12°; *c–c*$_2$ –14.5° (Green particles correspond to *1050A* aluminum, blue particles correspond to *321* steel)

For all studied conditions, a jet forms ahead of the collision point some time after the impact begins. In the initial impact zone, the interface is nearly flat. However, as the process develops, the deviation of the interface relief from an ideal line gradually increases. At all analyzed angles, the interface remains sharp, without significant material mixing.

At an impact angle of $\gamma = 9.5°$ (Fig. 2, *a–a2*), the deviations of the interface from flatness are weakly pronounced. The interface relief has a small amplitude and an almost symmetric shape. Relief formation occurs relatively slowly, which is attributed to insufficient shear deformation. At $\gamma = 12°$ (Fig. 2, *b–b2*), the most ordered interface relief is observed. The interface formation process is more intense than at 9.5°, indicating more favorable hydrodynamic conditions. At $\gamma = 14.5°$ (Fig. 2, *c–c2*), the wavy interface becomes asymmetric and oriented toward the more ductile aluminum. The onset of relief formation occurs earlier compared to 9.5° and 12°. However, at $t = 3.5$ µs (Fig. 2, *c2*), the interface shape becomes less regular, and isolated zones with local penetration of steel into aluminum appear. The formation of an asymmetric interface can be attributed to the development of shear instability [2, 26, 32]. As the impact angle increases, the tangential component of the impact velocity increases, causing intense mixing of the materials at the interface. With a higher shear velocity component, the plastic flow loses stability, leading to local asymmetric penetrations of the harder steel into the ductile aluminum. This interpretation is also consistent with the non-monotonic pressure dependence on impact angle.

Thus, increasing the impact angle from 9.5° to 14.5° accelerates the kinetics of relief formation, increases the wave amplitude, but reduces the regularity of the interface between the *1050A* aluminum and *321* stainless steel plates. The most ordered interface relief, which can be considered preferable for this material combination, forms at $\gamma = 12°$.

To verify the numerical model, explosive welding experiments were conducted on *1050A* and 321 plates at an impact angle of 12° and a collision point velocity V_c = 2,500 m/s. Fig. 3 shows a cross-section of the resulting joint. The results indicate that the interface is practically flat, without pronounced waves or macroscopic defects, which qualitatively corresponds to the computed morphology shown in Fig. 2, *b*. Thus, the proposed model correctly describes joint formation at this impact angle.

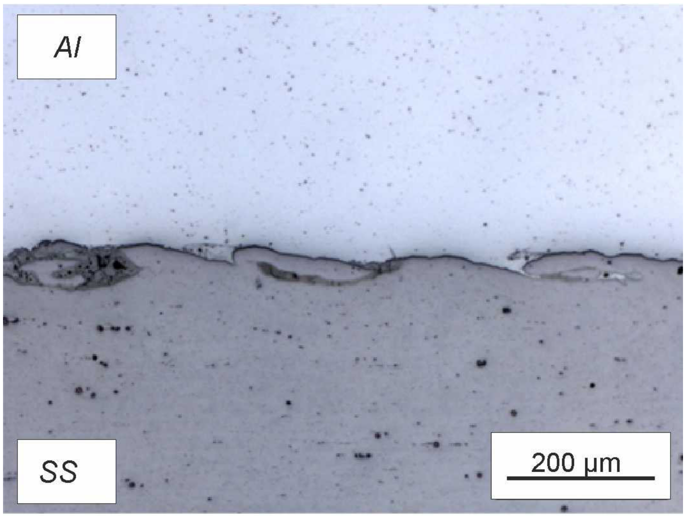

Fig. 3. Cross-section of the *1050A* / *321* explosively welded joint, obtained at $\gamma = 12°$ and V_c = 2,500 m/s (experiment)

Fig. 4 shows the distributions of pressure and temperature in the contact zone for the three impact angles at $t = 1.5$ µs. In all cases, high pressures and temperatures are localized along the plate interface, indicating the formation of a narrow intense interaction zone. As the impact angle increases from 9.5° to 14.5°, the recorded pressure and temperature values change as follows: at $\gamma = 9.5°$, pressure is 1.05 GPa and temperature is 1,026 K; at $\gamma = 12°$, pressure increases to 1.30 GPa and temperature to 1,120 K; at $\gamma = 14.5°$, pressure reaches 1.95 GPa and temperature 1,360 K. The increase in pressure with increasing

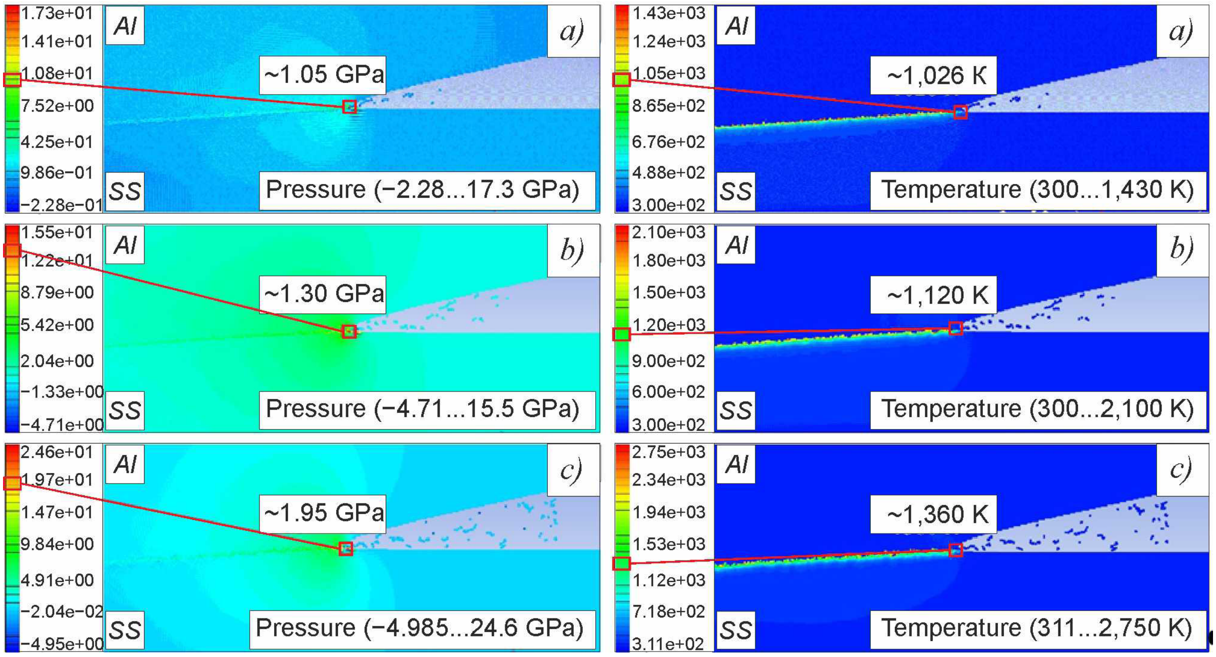

Fig. 4. Distribution of pressure and temperature in the contact zone of *1050A* and *321* plates during their collision at a time of 1.5 μs: (*a*) 9.5°, (*b*) 12°, (*c*) 14.5°

impact angle is due to the increase in the normal component of the impact velocity, which leads to more intense shock compression of the material at the collision point. The temperature rise, in turn, is a consequence of heating during high-strain-rate plastic deformation. In all considered cases, the temperature exceeds the melting point of aluminum (929 K), indicating local melting of the aluminum plate in the joint zone. At the same time, the temperature remains below the melting point of stainless steel (1,673 K), so no melting of the steel occurs. For $\gamma = 14.5°$, the temperature in the contact zone reaches 1,360 K, which can lead not only to melting of aluminum but also to significant softening of the steel near-surface layers, as well as create temperature–strain conditions favorable for possible diffusion and subsequent formation of intermetallic compounds.

The distributions of effective plastic strain and strain rate (Fig. 5) indicate localization of plastic flow in a narrow near-interface region. According to the data shown in Fig. 5, for $\gamma = 9.5°$, the effective plastic strain is 1.8, and the strain rate is 0.18 μs^{-1}; for $\gamma = 12°$, these values are 2.4 and 0.23 μs^{-1}, respectively; for $\gamma = 14.5°$ – 2.7 and 0.57 μs^{-1}. The highest strain value is recorded at $\gamma = 14.5°$, indicating more intense material flow in the impact zone as the angle increases [33, 34]. The increase in strain rate by more than a factor of three when transitioning from $\gamma = 9.5°$ to $\gamma = 14.5°$ is explained by the increase in the shear component of deformation, characteristic of oblique impacts. The high values of effective plastic strain (>2.0) and strain rate (~10^5–10^6 s^{-1}) ensure an adiabatic deformation conditions and the formation of an ultrafine-grained structure in the joint zone. However, at $\gamma = 14.5°$, the high shear strain may promote excessive heat release and increase the thickness of the intermetallic layer, which negatively affects the joint strength.

Analysis of the time dependences (Figs. 6, 7) allows refinement of the thermomechanical conditions of joint formation. Pressure reaches its maximum values in the time interval $t = 0.4$–0.6 μs after the start of impact for all analyzed angles. The highest pressure value (8.87 GPa) is recorded for $\gamma = 12°$ at $t = 0.429$ μs. For $\gamma = 9.5°$, the maximum pressure is 4.15 GPa at $t = 0.481$ μs, and for $\gamma = 14.5°$, the maximum pressure (7.71 GPa) is observed at $t = 0.385$ μs. Note that the pressure dependence on impact angle is non-monotonic. This may be because as the angle increases, the tangential component of the impact velocity increases, leading to more intense shear flow and possibly partial unloading of the material in the contact zone. A detailed non-monotonic dependence of pressure on impact angle has been noted in other studies [34, 35]. For example, *A.A. Akbari Mousavi* et al. [35] demonstrated that pressure increases as the impact angle rises from 8° to 11°, after which it decreases with a further increase to 15°.

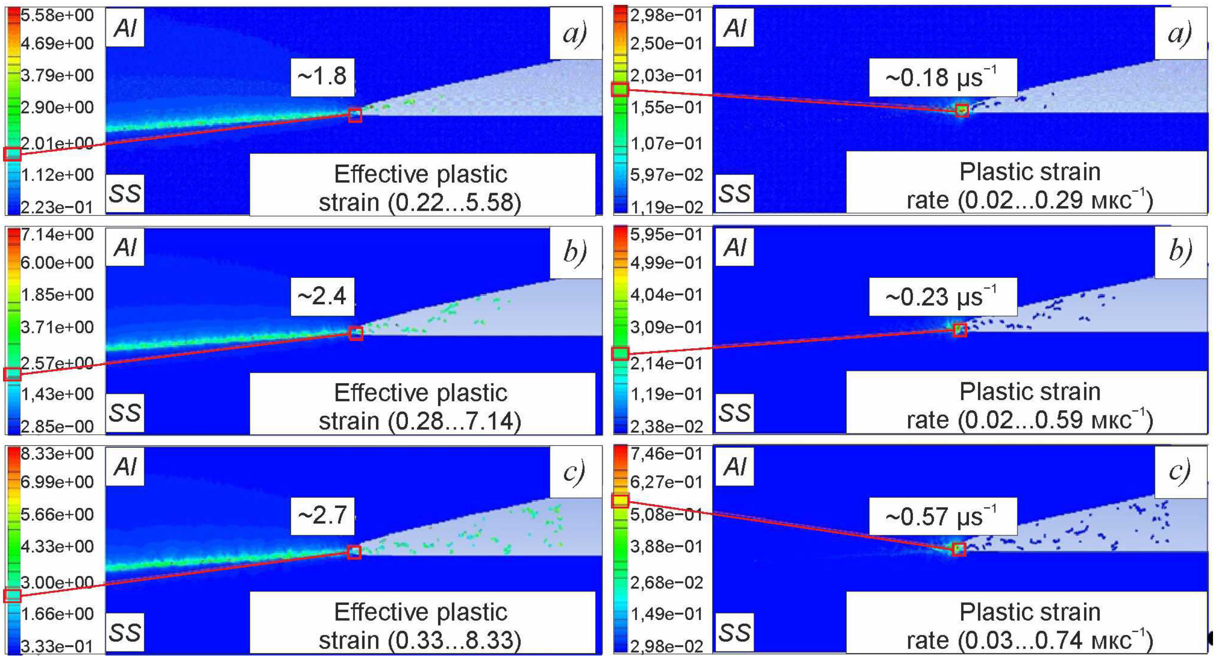

Fig. 5. Distribution of effective plastic strain and strain rate near the contact zone during collision of *1050A* and *321* plates at a time of 1.5 μs: (*a*) 9.5°, (*b*) 12°, (*c*) 14.5°

The temperature in the impact zone (Fig. 6) increases rapidly, reaches a maximum, and then decreases. The maximum temperature for **γ** = 12° reaches 1,314 K at ***t*** = 0.806 μs, and for **γ** = 14.5° – 1,372 K at ***t*** = 0.719 μs. In the latter case, the temperature rises more sharply, and after reaching the maximum, a rapid decrease is observed. At **γ** = 9.5°, the maximum temperature is 1,026 K (***t*** = 0.695 μs). Thus, increasing the impact angle to 14.5° promotes more intense heating but is accompanied by an accelerated temperature decrease, which may affect the joint structure formation.

The effective plastic strain (Fig. 7) varies non-monotonically with time, with alternating periods of increase and decrease, due to the passage of compression waves and subsequent material unloading. For **γ** = 14.5°, a value of 3.61 is reached as early as ***t*** = 0.554 μs, which is the highest value recorded over the entire simulation time interval. For **γ** = 12°, the maximum strain (3.31) is reached at ***t*** = 0.429 μs, and for **γ** = 9.5° – 2.01 (***t*** = 0.905 μs). This indicates that an increase in impact angle accelerates the onset of plastic flow, owing to the larger shear deformation component

The plastic strain rate (Fig. 7) reaches its highest values already in the initial moments of impact. For **γ** = 14.5°, the maximum strain rate is 2.79×10^6 s^{-1} (***t*** = 0.385 μs); for **γ** = 9.5° – 1.46×10^6 s^{-1} (***t*** = 0.481 μs); and for **γ** = 12° — 0.674×10^6 s^{-1} (***t*** = 0.429 μs). Overall, all recorded strain rate values exceed 10^5 s^{-1}, which is characteristic of high-velocity impact welding.

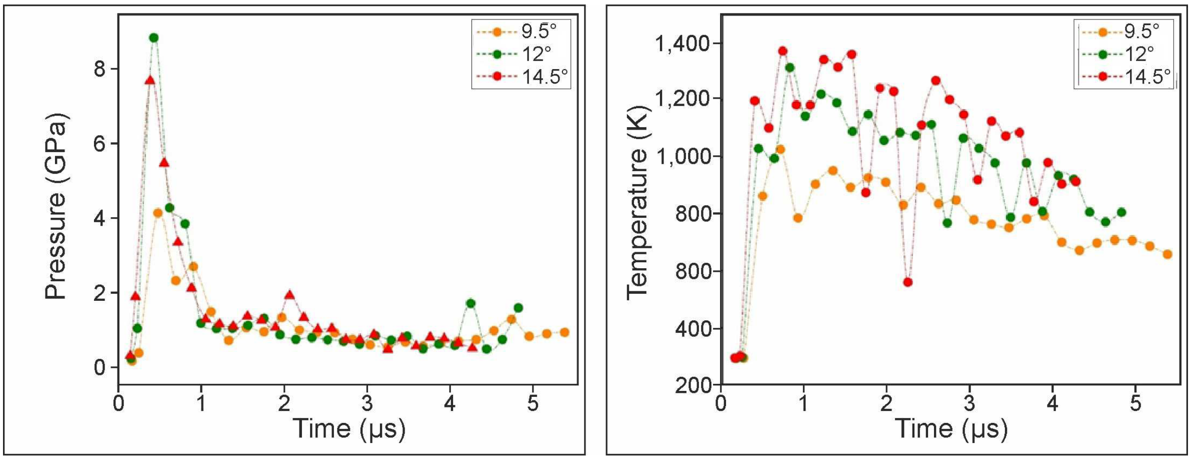

Fig. 6. Kinetics of pressure and temperature changes in the impact zone of *1050A* and *321* plates

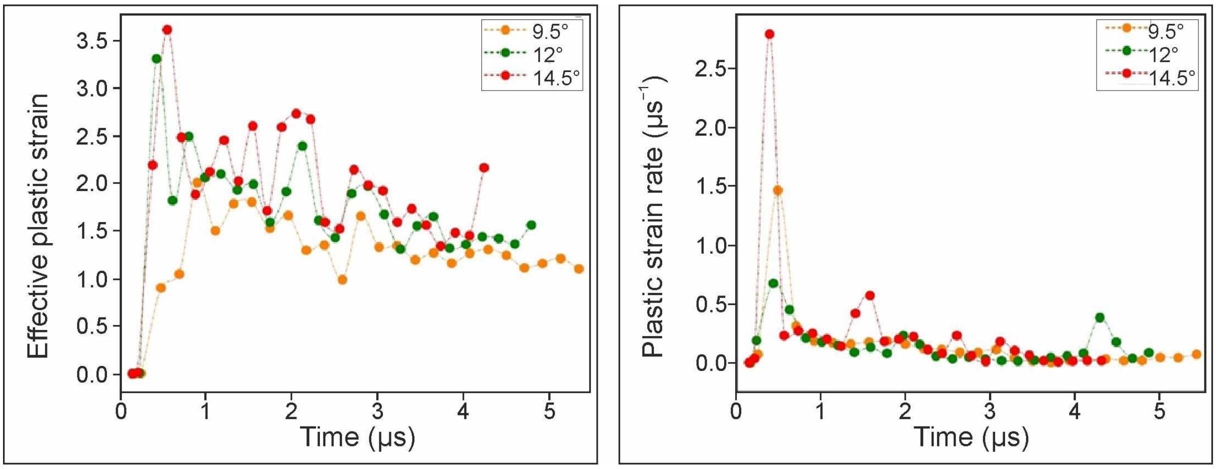

Fig. 7. Kinetics of changes in effective plastic strain and rate of plastic strain in the impact zone during explosion welding of the *1050A* / *321* plates

The numerical results obtained in the present study are in good agreement with previously reported data [33, 37]. According to references [38–40], for steel–aluminum bimetals, an impact angle in the range of 10–15° is considered most favorable, as it provides sufficient plastic deformation to achieve a strong bond without the formation of extensive intermetallic layers [38–40]. For a meaningful comparison of the investigated conditions, several criteria were adopted: contact pressure, temperature (high enough to induce local melting of aluminum but not excessive softening), and interface regularity. At an impact angle of 12°, the highest pressure was recorded, combined with a moderate temperature regime. Compared to impact angles of 9.5° and 14.5°, this suggests that an interface with minimal intermetallic layer thickness can be anticipated. Despite the higher temperature and strain values observed at 14.5°, excessive melting of aluminum may occur. As noted in [39, 41, 42], such overheating presents a risk of forming brittle intermetallic compounds.

The present simulation results indicate that the impact angle is a critical parameter governing heat generation and plastic deformation during explosive welding. Among the three impact angles examined, 12° is the most favorable for achieving a high-quality bond between *1050A* aluminum alloy and 321 stainless steel plates. At this angle, a high pressure is attained, and the maximum computed temperature in the joint zone (1,314 K at t = 0.806 μs) exceeds the melting point of aluminum (929 K) while remaining below that of stainless steel (1,673 K), thereby preventing melting of the steel. Due to the short duration of the process and the absence of prolonged high-temperature exposure, diffusion processes and intermetallic compounds growth are limited. This consequently promotes the formation of an interface with a minimal volume fraction of intermetallic-containing regions. However, it should be emphasized that determining the exact phase composition and thickness of the intermetallic layer will require additional experimental investigations, as well as simulations employing methods that account for diffusion processes, such as molecular dynamics [43].

Conclusions

1. Numerical simulations of the explosive welding process for the *1050A* / *321* bimetallic composite were conducted using the *SPH* method implemented in the *Ansys Autodyn* software. The calculations were performed at a constant collision point velocity V_c = 2,500 m/s and three impact angles: 9.5°, 12°, and 14.5°.

2. It was established that an increase in impact angle results in higher temperature, effective plastic strain, and strain rate in the joint zone, while pressure exhibits a non-monotonic dependence, reaching its maximum at γ = 12°. The highest values of temperature (1,372 K at t = 0.719 μs) and strain (3.61 at t = 0.554 μs) are attained at γ = 14.5°. However, this impact angle also leads to a sharp post-peak temperature decrease and the formation of an asymmetric wavy interface characterized by steel penetration into aluminum.

3. Under all investigated conditions, the temperature in the contact zone exceeds the melting point of aluminum but remains below the melting point of steel. This indicates local melting of the aluminum workpiece while the steel remains in the solid state.

4. The most regular interface is formed at an impact angle of γ = 12°. At this angle, the highest pressure (8.87 GPa at t = 0.729 μs) is recorded. Moderate heating combined with a high degree of plastic deformation creates favorable conditions for the formation of a high-quality joint with minimal intermetallic layer thickness.

5. Analysis of the temperature–strain characteristics and interface morphology demonstrates that the impact angle of 12° is the most favorable among those studied for explosive welding of the *1050A* / *321* composite. This processing condition (γ = 12°, V_c = 2,500 m/s) is recommended for producing bimetallic joints with high strength and minimal content of brittle intermetallic compounds.

References

1. Kuzmin V.I., Lysak V.I., Tupitsin M.A. Issledovanie zakonomernostei obrazovaniya soedineniya pri svarke vzryvom tolstolistovykh stalealyuminievykh kompozitov [An investigation of the mechanism of steel–al joint formation under explosion welding of composite plates]. *Fizika i khimiya obrabotki materialov = Physics and Chemistry of Materials*, 2013, no. 3, pp. 64–69. (In Russian).

2. Deribas A.A. *Fizika uprochneniya i svarki vzryvom* [Physics of hardening and explosive welding]. Novosibirsk, Nauka Publ., 1980. 224 p.

3. Aceves S.M., Espinosa-Loza F., Elmer J.W., Huber R. Comparison of Cu, Ti and Ta interlayer explosively fabricated aluminum to stainless steel transition joints for cryogenic pressurized hydrogen storage. *International Journal of Hydrogen Energy*, 2015, vol. 40 (3), pp. 1490–1503. DOI: 10.1016/j.ijhydene.2014.11.038.

4. Lienert T., Siewert T., Babu S., Acoff V., eds. *ASM Handbook. Vol. 6A. Welding Fundamentals and Processes*. ASM International, 2011. 912 p. ISBN 978-1-61503-001-9.

5. Chadwick M.D., Jackson P.W. Explosive welding in planar geometries. *Explosive welding, forming and compaction*. Dordrecht, Springer Netherlands, 1983, pp. 219–287.

6. Findik F. Recent developments in explosive welding. *Materials & Design*, 2011, vol. 32 (3), pp. 1081–1093. DOI: 10.1016/j.matdes.2010.10.017.

7. Zlobin B.S. Explosion welding of steel with aluminum. *Combustion, Explosion, and Shock Waves*, 2002, vol. 38, pp. 374–377. DOI: 10.1023/A:1015674407898.

8. Chu Q., Xia T., Zhao P., Zhang M., Zheng J., Yan F., Cheng P., Yan C., Liu C., Luo H. Interfacial investigation of explosion-welded Al/Steel plate: the microstructure, mechanical properties and residual stresses. *Materials Science and Engineering: A*, 2022, vol. 833, art. 142525. DOI: 10.1016/j.msea.2021.142525.

9. Hokamoto K., Izuma T., Fujita M. New explosive welding technique to weld aluminum alloy and stainless steel plates using a stainless steel intermediate plate. *Metallurgical Transactions A*, 1993, vol. 24, pp. 2289–2297. DOI: 10.1007/BF02648602.

10. Li X., Ma H., Shen Z. Research on explosive welding of aluminum alloy to steel with dovetail grooves. *Materials and Design*, 2015, vol. 87, pp. 815–824. DOI: 10.1016/j.matdes.2015.08.085.

11. Kuz'min V.I., Lysak V.I., Strokov O.V., Litvinov V.V. *Issledovanie termostoikosti kompozitsionnogo stalealyuminievogo materiala i puti ee povysheniya* [Study of the heat resistance of composite steel-aluminum material and ways to improve it]. *Perspektivnye materialy = Journal of Advanced Materials*, 2007, no. 5, pp. 78–81. (In Russian).

12. Gurevich L.M., Pronichev D.V., Trudov A.F., Trykov Yu.P., Trunov M.D. Issledovanie vliyaniya rezhimov svarki vzryvom i termicheskoi obrabotki na strukturu i svoistva bimetalla AD1-stal' St3 [Investigation of the influence of explosive welding modes and heat treatment on the structure and properties of AD1–St3 steel bimetal]. *Izvestiya Volgogradskogo gosudarstvennogo tekhnicheskogo universiteta = Izvestia of Volgograd State Technical University*, 2014, no. 9, pp. 17–21.

13. Shargh S.F., Saadat A., Najafi A., Gharehshiran M.-R.K., Khalaj G. Investigating the effect of post weld heat treatment on corrosion properties of explosive bonded interface of AA5083/AA1050/SS 321 tubes. *Materials Research Express*, 2020, vol. 7, art. 036529. DOI: 10.1088/2053-1591/ab8095.

14. Jandaghi M.R., Pouraliakbar H., Moverare J., Fallah V., Khalaj G. Design of explosively welded Fe–Al multilayer laminated composite pipes: a critical microscopy analysis of stand-off distance and post-weld heat

treatment effects on interface properties. *Journal of Materials Research and Technology*, 2024, vol. 33, pp. 2645–2660. DOI: 10.1016/j.jmrt.2024.10.003.

15. Tricarico L., Spina R., Sorgente D., Brandizzi M. Effects of heat treatments on mechanical properties of Fe/Al explosion-welded structural transition joints. *Materials and Design*, 2009, vol. 30, pp. 2693–2700. DOI: 10.1016/j.matdes.2008.10.010.

16. Grignon F., Benson D., Vecchio K.S., Meyers M.A. Explosive welding of aluminum to aluminum: analysis, computations and experiments. *International Journal of Impact Engineering*, 2004, vol. 30 (10), pp. 1333–1351. DOI: 10.1016/j.ijimpeng.2003.09.049.

17. Nguyen V.-T., Nhu T.T.V., Vo X.-T., Van Huong H. Atomistic simulation into Cu–Al explosive welding joint formation mechanisms and deformation characteristics. *Physica B: Condensed Matter*, 2025, vol. 705, art. 417084. DOI: 10.1016/j.physb.2025.417084.

18. Pai V.V., Titov V.M., Luk'yanov Ya.L., Zubashevskii K.M. Izmerenie temperatury kumulyativnoi strui iz konicheskoi oblitsovki [Temperature measurement of the shaped-charge jet from a conical liner]. *Fizika goreniya i vzryva = Combustion, Explosion, and Shock Waves*, 2020, vol. 56, no. 3, pp. 123–126. DOI: 10.15372/FGV20200313. (In Russian).

19. Bataev I.A., Tanaka S., Zhou Q., Lazurenko D.V., Junior A.M.J., Bataev A.A., Hokamoto K., Mori A., Chen P. Towards better understanding of explosive welding by combination of numerical simulation and experimental study. *Materials and Design*, 2019, vol. 169, art. 107649. DOI: 10.1016/j.matdes.2019.107649.

20. Bataev I.A. Formirovanie struktury svarennykh vzryvom materialov: eksperimental'nye issledovaniya i chislennoe modelirovanie [Structure of explosively welded materials: experimental study and numerical simulation]. *Obrabotka metallov (tekhnologiya, oborudovanie, instrumenty) = Metal Working and Material Science*, 2017, vol. 19, no. 4, pp. 55–67. DOI: 10.17212/1994-6309-2017-4-55-67.

21. Kiselev S.P., Kiselev V.P., Kiselev N.P., Zaikovskii V.N. O modeli volnoobrazovaniya pri kosom, simmetrichnom soudarenii alyuminievykh plastin [On the model of wave formation during oblique, symmetrical collision of aluminum plates]. *Fizika goreniya i vzryva = Combustion, Explosion, and Shock Waves*, 2025. DOI: 10.15372/FGV2025.9600. (In Russian).

22. Bataev I., Mori A., Hokamoto K. Behavior of materials under extremely high-velocity oblique impact. *Explosion, Shock-wave and High-strain-rate Phenomena of Advanced Materials*. Elsevier, 2021, pp. 71–92. DOI: 10.1016/B978-0-12-821665-1.00006-7.

23. Tanaka K. Numerical studies on the explosive welding by smoothed particle hydrodynamics (SPH). *Shock Compression of Condensed Matter – 2007: Proceedings of the American Physical Society Topical Conference. AIP Conference Proceedings*, vol. 955. Melville, NY, AIP, 2008, pp. 1301–1304. DOI: 10.1063/1.2832962.

24. Chen X., Inao D., Tanaka S., Li X., Bataev I.A., Hokamoto K. Comparison of explosive welding of pure titanium/SUS 304 austenitic stainless steel and pure titanium/SUS 821L1 duplex stainless steel. *Transactions of Nonferrous Metals Society of China*, 2021, vol. 31 (9), pp. 2687–2702. DOI: 10.1016/S1003-6326(21)65685-6.

25. Wang X., Zheng Y., Liu H., Shen Z., Hu Y., Li W., Gao Y., Guo C. Numerical study of the mechanism of explosive/impact welding using Smoothed Particle Hydrodynamics method. *Materials and Design*, 2012, vol. 35, pp. 210–219. DOI: 10.1016/j.matdes.2011.09.047.

26. Crossland B. *Explosive welding of metals and its application*. Oxford, Clarendon Press, 1982. 256 p. ISBN 0-19-859119-5.

27. Yang M., Chen D., Zhou H., Xu J., Ma H., Shen Z., Zhang B., Tian J. Experimental and numerical investigation of microstructure and evolution of TiNi alloy/Q235 steel interfaces prepared by explosive welding. *Journal of Materials Research and Technology*, 2021, vol. 15, pp. 5803–5813. DOI: 10.1016/j.jmrt.2021.11.044.

28. Zhang B., Ma H., Xu J., Li L., Shen Z., Ding L., Tian J. Investigations on the microstructure evolution and mechanical properties of explosive welded ODS-Cu/316L stainless steel composite. *Fusion Engineering and Design*, 2022, vol. 179, art. 113142. DOI: 10.1016/j.fusengdes.2022.113142.

29. Ma Y., Wang T., Wang G., Fang X., Chu C. Numerical and experimental studies of the interface characteristics and wave formation mechanism of Hastelloy/stainless steel explosive welding composite plate. *Materials Today Communications*, 2023, vol. 36, art. 106880. DOI: 10.1016/j.mtcomm.2023.106880.

30. Wu X., Shi C., Feng K., Gao L., Li W., Qian K. Experimental and numerical approach to titanium-aluminum explosive welding. *Materials Research Express*, 2021, vol. 8, art. 096503. DOI: 10.1088/2053-1591/ac2017.

31. Campanella D., Buffa G., Fratini L. A two steps Lagrangian–Eulerian numerical model for the simulation of explosive welding of three dissimilar materials joints. *CIRP Journal of Manufacturing Science and Technology*, 2021, vol. 35, pp. 541–549. DOI: 10.1016/j.cirpj.2021.08.010.

32. Ryabinkina P.A., Emurlaeva Yu.Yu., Bataev I.A., Tanaka S. Neodnorodnost' plasticheskogo techeniya, soputstvuyushchaya protsessam vysokoskorostnogo nagruzheniya metallicheskikh materialov [Inhomogeneity of plastic flow accompanying rapid loading of metallic materials]. *Metallovedenie i termicheskaya obrabotka metallov = Metal Science and Heat Treatment*, 2021, no. 12, pp. 41–47. DOI: 10.30906/mitom.2021.12.41-47. (In Russian).

33. Hokamoto K., Ujimoto Y., Fujita M. Basic characteristics of the explosive welding technique using underwater shock wave and its possibilities. *Materials Transactions*, 2004, vol. 45 (9), pp. 2897–2901. DOI: 10.2320/matertrans.45.2897.

34. Akbari Mousavi A.A., Al-hassani S. Numerical and experimental studies of the mechanism of the wavy interface formations in explosive/impact welding. *Journal of the Mechanics and Physics of Solids*, 2005, vol. 53, pp. 2501–2528. DOI: 10.1016/j.jmps.2005.06.001.

35. Wu X. , Shi Ch., Gao L., Li W., Feng K. Study on parameters and wave growth mechanism of explosive welding based on SPH-FEM. Rare Metal Materials and Engineering, 2023, vol. 52 (4), pp. 1272–1282.

36. Besshaposhnikov Yu.P., Grinberg B.A., Pushkin M.S., Inozemtsev A.V., Patselov A.M. Optimizatsiya parametrov svarki vzryvom i strukturnye osobennosti kompozitov stal' – tolstolistovoi alyuminii [Optimization of explosive welding parameters and structural features of steel–thick aluminum composites]. *Fundamental'nye problemy sovremennogo materialovedeniya = Basic Problems of Material Science*, 2022, vol. 19, no. 3, pp. 362–375. DOI: 10.25712/ASTU.1811-1416.2022.03.009.

37. Carvalho G.H.S.F.L., Galvão I., Mendes R., Leal R.M., Loureiro A. Formation of intermetallic structures at the interface of steel-to-aluminium explosive welds. *Materials Characterization*, 2018, vol. 142, pp. 432–442. DOI: 10.1016/j.matchar.2018.06.005.

38. Wang J., Li X., Yan H., Wang X., Wang J. Investigation of crack control mechanisms for intermetallic compounds at the interface of aluminum/steel during explosive welding. *Transactions of the Indian Institute of Metals*, 2025, vol. 78, art. 121. DOI: 10.1007/s12666-025-03582-2.

39. Aizawa Y., Nishiwaki J., Harada Y., Muraishi S., Kumai S. Experimental and numerical analysis of the formation behavior of intermediate layers at explosive welded Al/Fe joint interfaces. *Journal of Manufacturing Processes*, 2016, vol. 24, pp. 100–106. DOI: 10.1016/j.jmapro.2016.08.002.

40. Szecket A., Inal O.T., Vigueras D.J., Rocco J. A wavy versus straight interface in the explosive welding of aluminum to steel. *Journal of Vacuum Science and Technology A*, 1985, vol. 3 (6), pp. 2588–2593. DOI: 10.1116/1.572839.

41. Kuz'min S.V., Lysak V.I., Ribin V.V., Peev A.P. Osobennosti plasticheskoi deformatsii metalla okoloshovnoi zony pri svarke vzryvom raznorodnykh materialov [Features of plastic deformation of steel in the heat-affected zone during explosion welding of dissimilar metals]. *Izvestiya Volgogradskogo gosudarstvennogo tekhnicheskogo universiteta = Izvestia of Volgograd State Technical Universit*, 2010, vol. 5, no. 65, pp. 4–11.

42. Chen S.Y., Wu Z.W., Liu K.X., Li X.J., Luo N., Lu G.X. Atomic diffusion behavior in Cu–Al explosive welding process. *Journal of Applied Physics*, 2013, vol. 113, art. 044901. DOI: 10.1063/1.4775788.

43. Zhou J., Luo N., Liang H., Sun W. Multi-scale simulation and microstructure characteristics of TC4 ELI/Al 6013 plates by explosive welding. *Journal of Manufacturing Processes*, 2024, vol. 124, pp. 1180–1192. DOI: 10.1016/j.jmapro.2024.07.014.

Conflicts of Interest

The authors declare no conflict of interest.